80th
ANNIVERSARY OF
PARÍCUTIN VOLCANO

FIELD GUIDE FOR THE HORSE-RIDE TRAIL TO PARÍCUTIN VOLCANO

Wednesday, February 22, 2023

GUÍA DE CAMPO AL VOLCÁN PARÍCUTIN POR LA RUTA A CABALLO

Miércoles 22 de febrero de 2023

Xavier Bolós[1], Patricia Larrea[2], Marie-Noëlle Guilbaud[3], Sergio Salinas[4], Claus Siebe[3]

1) Department of Mineralogy, Petrology and Applied Geology, Earth Sciences Faculty, University of Barcelona, Martí i Franquès s/n 08028, Barcelona, Catalonia, Spain. xavier.bolos@gmail.com
2) Departamento de Geología, Facultad de Ciencias Físicas y Matemáticas, Universidad de Chile, Santiago, Chile. patricia.larrea@uchile.cl
3) Departamento de Vulcanología, Instituto de Geofísica, Universidad Nacional Autónoma de México, Mexico City. marie@igeofisica.unam.mx; csiebe@geofisica.unam.mx
4) División de Ingeniería en Ciencias de la Tierra, Facultad de Ingeniería, Universidad Nacional Autónoma de México. sss@geofisica.unam.mx

Abstract

Parícutin volcano in western-central Mexico is one of the most significant geosites in the country. Parícutin erupted between 1943 and 1952 and is the youngest volcano of the Michoacán-Guanajuato Volcanic Field together with Jorullo (1759-1774). Both of them are the unique monogenetic volcanoes formed since the Spanish conquest (1519-1521) in the Trans-Mexican Volcanic Belt. As part of the activities related to the 80th anniversary celebration of the Parícutin eruption, we organized this one-day excursion to the Parícutin volcano. Horses are the easiest and most rapid means to reach the base of the cone. Thus, in this field trip, we will get to the volcano by riding horses. We will depart from the town of Angahuan, surround the lava field on its western side, and cross the ash deposits that erupted during the explosive phases of the eruption. After reaching the base of the scoria cone, we will dismount and secure the horses under a shade, and climb to the crater rim. The path is ~11 km long and it takes ~4 hours from Angahuan to the crater's summit. Then, we will trot back to Angahuan, and pay on our way a visit to the church ruins of San Juan Parangaricutiro, where will have the opportunity to enjoy the most delicious "quesadillas" in the world.

Resumen

El volcán Parícutin en el centro-oeste de México es uno de los geositios más importantes del país. Parícutin entró en erupción entre 1943 y 1952, siendo así el volcán más joven del Campo Volcánico Michoacán-Guanajuato junto con Jorullo (1759-1774). Ambos, son los únicos volcanes monogenéticos formados desde la conquista española (1519-1521) en el Cinturón Volcánico Trans-mexicano. Como parte de las actividades por la celebración del 80 aniversario de la erupción del Parícutin, organizamos esta excursión de un día hasta el volcán Parícutin. Los caballos son el medio más fácil y rápido para llegar a la base del cono. Así, en esta excursión, llegaremos al volcán a caballo desde el pueblo de Angahuan, bordeando el campo de lava y atravesando los depósitos de ceniza emitidos durante las fases explosivas de la erupción. Tras llegar a la base del cono de escoria, desmontaremos y aseguraremos los caballos bajo la sombra, y luego subiremos a la cumbre. El camino es de ~11 km, alrededor de 4 horas desde Angahuan hasta la cima del cráter. Luego, regresamos trotando a Angahuan, visitando en el camino las ruinas de la iglesia de San Juan Parangaricutiro con la posibilidad de comer las quesadillas más deliciosas del mundo.

Introduction

This field trip was designed as a 1-day excursion offered to participants of the conference commemorating the 80th anniversary of the Parícutin (February 19-24, 2023). Parícutin is located in the Purépecha region and can be easily reached on paved roads from Morelia, the capital city of the state of Michoacán in Mexico (Figs. 1 and 2). The small picturesque town of Angahuan is the closest to the volcano (Fig. 2) and the place where we will start the horse-ride trail. It is located 23 km NW of the city of Uruapan, which announces itself as the “world capital of avocado”. Uruapan can be reached from Morelia after a drive of 111 km (~1:30 hour) by taking the new toll road via Pátzcuaro. Hosting facilities are very limited in Angahuan (cabins at Angahuan Tourist Center) but Uruapan offers multiple options for accommodation. The area is characterized by pine-and-oak forests and plantations of avocado trees. Temperatures at night can be relatively cold in the Parícutin area due to high altitudes (2400 masl at Angahuan, and 2770 masl at the summit of the Parícutin cone). Angahuan and other towns in the area are inhabited by Purhépecha indigenous communities, many of which still speak their native language.

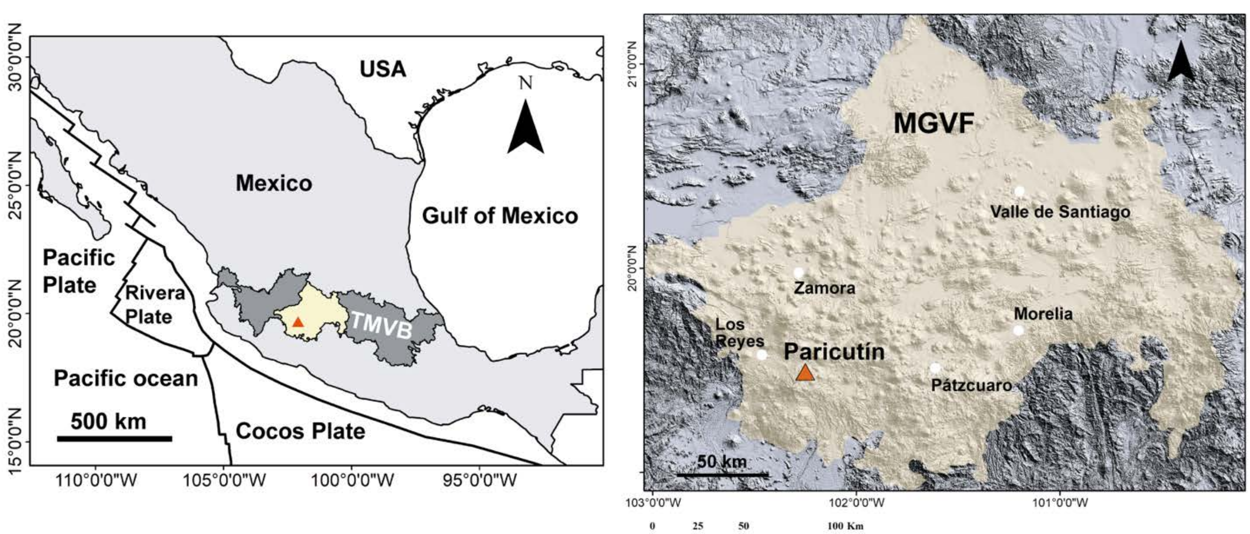

Figure 1: The left map shows the location of the MGVF within the trans-Mexican Volcanic Belt (TMVB). The right map is a DEM of the Michoacán–Guanajuato volcanic field (MGVF, yellow area) showing the location of Parícutin volcano (red triangle) and the main towns (white dots).

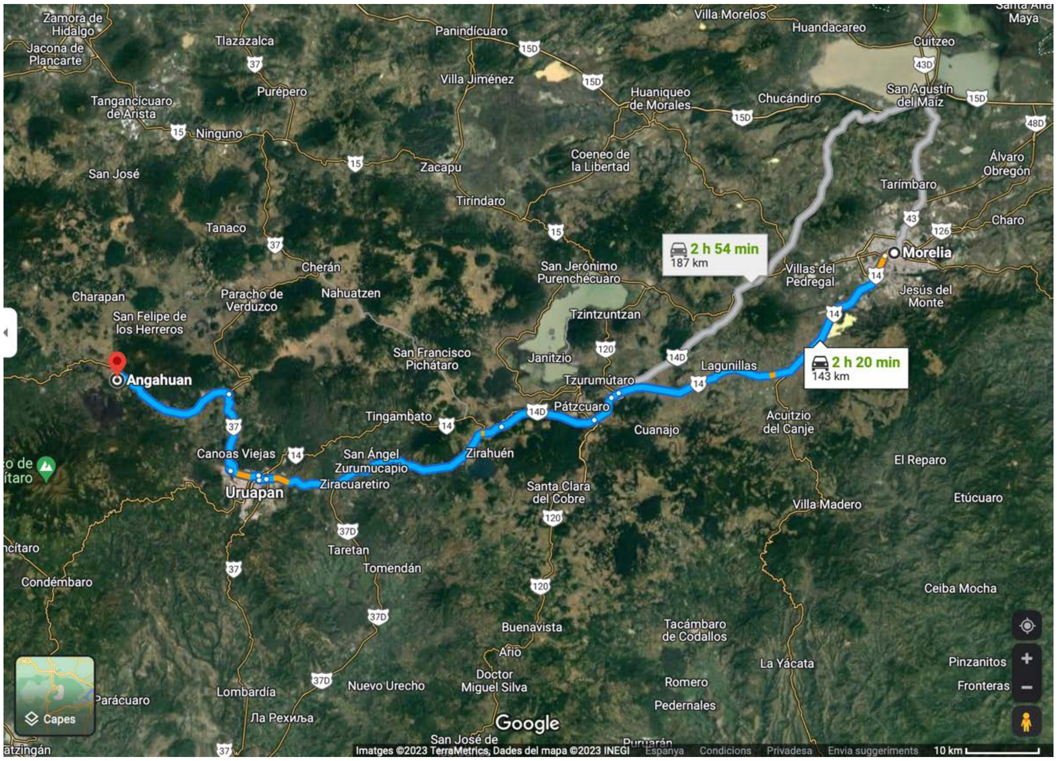

Figure 2: Road map of the itinerary from Morelia to Angahuan, showing main cities and towns (Google Maps).

This field guide follows on and is an update of two previous guides (Guilbaud et al, 2009; Siebe et al., 2014), which focused on several volcanic sites of the Michoacán-Guanajuato Volcanic Field, including the Parícutin area. We note that the volcano cannot be reached by a paved road and is surrounded by a field of irregular lavas so that horses are the easiest and most rapid means to reach the base of the cone. Thus, in this field trip, we will get to the volcano by going around the lavas to the west and crossing through the ash deposits that erupted during the explosive phases of the eruption. We will then get off the horses and climb the cone. After running down the cone´s slopes, we will trot back to Angahuan, making a stop at the church ruins of San Juan Parangaricutiro, before reaching the town of Angahuan.

Geological setting and regional volcanic activity

The Michoacán-Guanajuato Volcanic Field in the Trans-Mexican Volcanic Belt is one of the largest monogenetic fields related to a continental arc on Earth, holding more than 1,200 edifices (Hasenaka and Carmichael, 1985; Valentine and Connor, 2015; Mahgoub et al., 2017). This volcanic field contains abundant scoria cones, about 300 "enigmatic" small shields, ~25 maar-craters, and two old and poorly studied stratovolcanoes, Tancítaro and Patambán (Ownby et al., 2007; Siebe et al., 2014). Parícutin (1943-1952) is the youngest volcano of this field and together with Jorullo (1759-1774) the only monogenetic volcanoes formed since the Spanish conquest (1519-1521) in the Trans-Mexican Volcanic Belt. However, another monogenetic eruption will certainly occur again in this volcanic field. Over the last twenty years, several seismic swarms occurred nearby the Tancítaro-Parícutin region (1997, 1999, 2000, 2006, 2020 and 2021) (Gardine et al 2011; Jácome et al., 2022). For that reason, a monitoring system has been recently set up in the Parícutin area, which provided crucial information on the last 2020 and 2021 seismic swarms. This system has detected about 100,000 earthquakes (Perton, personal communication, 2022), which are interpreted to be the result of dykes opening by hydraulic fracture in a fragile domain (< 15 km depth). In order to minimize the loss of life and property it is necessary to learn more about this type of eruptions and their preceding unrest phenomena. Only then will we be able to anticipate an eruption and design better preventive strategies for the mitigation of its hazards.

The Parícutin eruption

The Parícutin eruption was witnessed initially by local inhabitants, and later by scientists. This volcano, which erupted in the middle of a cornfield, has become one of the best-known monogenetic volcanoes in the world (Fig. 3). Its eruption dynamics and magma composition have been described in numerous papers, based on the detailed accounts of the local people, visitors, and scientists who witnessed the eruption from the early beginning to its end, providing an invaluable detailed record of a monogenetic eruption.

Figure 3: Parícutin eruption (photo by Hugo Brehme).

The eruption started on February 20, 1943 and ended on March 4, 1952 (Wilcox, 1954). It produced ~ 2.5 km^3 of material (dense rock equivalent), including 0.89 km^3 of tephra forming the cone and the ash blanket (Fries, 1953), and 1.64 km^3 of lava (Larrea et al., 2017). The onset of activity was preceded by 45 days of enhanced regional seismicity. The birth of the volcano was witnessed by at least four local people, including the owner of the cornfield. The volcano first formed a E-W-oriented fissure in alluvium that emitted ash, sulfur-rich gases, and incandescent bombs. A main cone grew rapidly, reaching 148 m in height at the end of the first month. Explosive activity was intense and often associated with lava effusion from separate vents. It was described as “violent Strombolian” (MacDonald, 1972; Pioli et al., 2008). Eruptive clouds reached up to 8 km in height and fine ash fell on distant places, including Mexico City (350 km to the east) during the first days of April 1943. The intensity of the explosive activity and the volume of lava and tephra erupted, decreased gradually during the eruption as the magma flux declined (Fries, 1953).

Throughout the entire duration of the eruption, a cast of scientists (Adán Pérez-Peña, Jenaro González-Reyna, Ezequiel Ordóñez, William Foshag, Konrad Krauskopf, Kenneth Segerstrom, Howel Williams, Ray Wilcox, etc.) surveyed the progression of the eruption and provided maps depicting the volcano's sequential growth. They collected in-situ samples of the emitted tephras and lavas, took photographs, and partially filmed the eruption during the nine years of eruptive activity. Later, this information together with testimonies by eyewitnesses were compiled by James Luhr and Tom Simkin in a review book (Luhr et al., 1993) that is considered the best documentation of the formation and evolution of the Parícutin volcano. Based on eruptive dynamics and chemo-stratigraphic features of its products, this eruption has been divided by several authors into three main stages: Stage I (1943); Stage II (1943-1946); and Stage III (1947-1952) (Luhr, 2001; Pioli et al., 2008; Erlund et al., 2010; Rowe et al., 2011; Bolós et al., 2021). The emitted tephra and lava products evolved with time from basaltic andesite to andesite (53–60.5 wt.% SiO_2) (Larrea et al., 2019). Several studies dealing with the petrology and geochemical characteristics of lavas, tephra, and xenoliths, together with melt inclusion studies, proposed that crustal contamination was an important process in the petrogenesis of Parícutin’s magmas (e.g., Wilcox, 1954; McBirney et al., 1987; Luhr, 2001; Erlund et al., 2010; Cebriá et al., 2011; Rowe et al., 2011). These studies led to the notion of Parícutin representing a classic example of assimilation-fractional crystallization (AFC) in a subduction calc-alkaline setting. A multi-isotopic study of Parícutin products by Larrea et al. (2019), revealed that the compositional variations are inconsistent with significant crustal assimilation. Alternatively, Parícutin’s geochemical variability is explained by a combination of variable degrees of fractional crystallization of magmas produced by melting heterogeneous mantle metasomatized by subduction components (Larrea et al., 2019). In addition, recent mineral chemistry and olivine diffusion timescales studies by Albert et al. (2020), and Larrea et al. (2021), revealed the existence of a convective magma regime during the first weeks/months of the eruption (“opening stage”), with large temperature and oxygen fugacity gradients characterized by short timescales (few days), followed by a steadier magma regime with longer timescales (few months) and including periodic magma recharge, mixing, and fractional crystallization.

The eruption had important social and economic impacts as two villages, San Juan Parangaricutiro (4000 inhabitants) and Parícutin (733 inhabitants), and a total of 24.8 km^2 of land were buried under lava (Luhr et al., 1993). The vegetation was completely destroyed within an area of 300 km^2 as it was covered by more than 15 cm of ash, which affected greatly the ecology and agriculture (Luhr et al., 1993). Moreover, three years after the eruption began (1946)—as identified by Segerstrom (1950) — several types of erosion affected the pyroclastic deposits, such as: creeping, landslides, mud-flows, water erosion (e.g., erosion grooves), and wind erosion (e.g., ripples and dunes). Mass wasting and water erosion occurred mainly during the rainy season, which lasts from May to October, eventually producing major lahars that flooded toward the NW through the town of Los Reyes (Segerstrom, 1950, 1960). In comparison, wind erosion acted primarily in the dry season, the period from November to April. The interaction of these external factors with ash fall deposits generated complex interbedding of deposits. Therefore, the Parícutin eruption and its related sediments provide a good example of the wide range of syn- and post-depositional sedimentary processes related to ash-rich eruptions.

Parícutin horse-ride trail and geo-stops

This fieldtrip starts at the visitor center of Angahuan. The path used to get to the cone rim is ~11 km long and takes ~4 hours (Fig. 4).

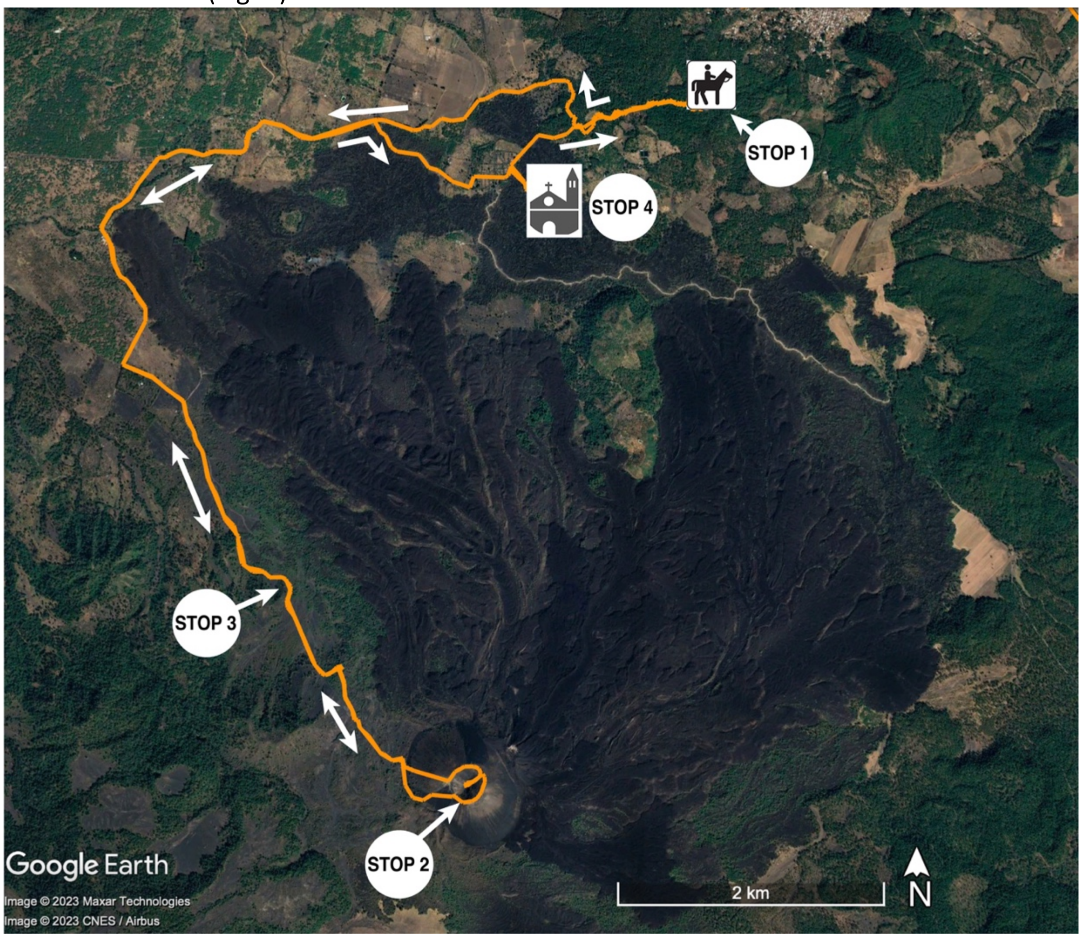

Figure 4: Horse trail to Parícutin volcano from the town of Angahuan (Aerial view from Google Earth).

The first stop is a panoramic view of Parícutin and its lava flow-field from a terrace in front of a cafeteria in the Angahuan Tourist Center (Fig. 5).

Figure 5: Panoramic view of Parícutin cone and Sapichu lateral vent from the Angahuan Tourist Center.

After a horse-ride of ~3 hours, we reach the western base of the cone. Then, after dismounting and securing the horses under the shade of a group of pine trees, the cone can be climbed in 30 to 60 minutes, following a path that goes diagonally to the S crater rim and around the crater (Stop 2 - Fig. 4). The climb is somewhat tedious, because of the loose scoria and ash that form the slopes. The descent is much faster and starts from the main summit on the W crater rim and goes straight down to the groove of trees where the horses were left behind. Consider that on the crater rim the wind is often strong (watch your *sombrero*) and temperatures are fresh (bring your jacket) as the summit culminates at ~2800 masl.

The cone is 220 m high and 950 m wide at the base. The crater has a diameter of 250 m and a depth of ~40 m. The evolution of the cone during the eruption is well documented (see Luhr and Simkin, 1993). It grew mostly during the first year. By the end of the first day, it was already 30 m high (nearly 1 m/ hr), doubled in height by the end of the third day, and reached 148 m in height at the end of the first month (average of 5 m/day). By the end of the first year, it was 336 m high (almost 1 m/day on average). In the following 8 years it grew slowly, finally reaching its maximum height of 424 m in 1952. Note that lava flows covered the base so that the height of the cone protruding from the flows is lower (220 m) than its actual height (424 m, see above).

The cone growth was not continuous. Eyewitnesses describe several episodes of partial destruction (e.g., Ordóñez, 1947; Foshag and González-Reyna, 1956). Sector collapses were accompanied by lateral lava outbreaks. At the beginning of the eruption, lava emerged from vents formed within the cone and flowed out from the opening in the cone left by the collapse (Fig. 6). Later in the eruption, when the cone had reached maturity, lava was emitted from temporary vents formed at the base of the cone (Fig. 6).

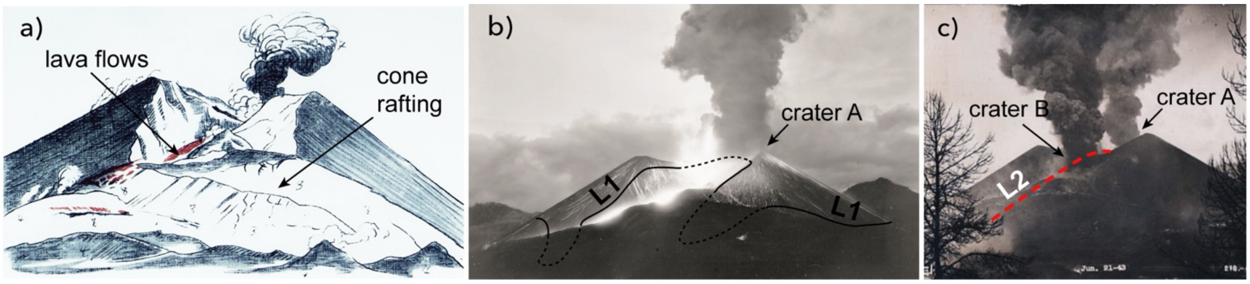

Figure 6: (a) Sector collapse during Stage I of the eruption, as observed and painted in the tonal drawing by Dr. Atl (1950) (14 June 1943). b) Lava flows after the cone sector collapse on 20 June 1943, displaying the L1 lineament (photo by R. Garcia). (c) Two eruptive columns rise from A and B craters aligned with the L2 lineament; photo taken on 21 June 1943 by an anonymous photographer.

During pauses in lava emission or changes in the vent location, explosive activity at the cone rapidly healed the breaches, restoring the cone's symmetry (Luhr et al., 1993; Foshag and González-Reyna, 1956). It is remarkable that the current shape of the cone does not record any of these episodes of destruction and reconstruction (Fig. 7). However, recent geophysical surveys revealed the morphology of a buried horseshoe-shaped crater produced by cone collapse early in the eruption, as well as the contact between lava flows and the overlying pyroclastic fallout deposits (Fig. 8) (Bolós et al., 2020). Moreover, the use of these geophysical methods allowed also inferring the cone's evolution, describing the geometry of the eruption's feeder dyke and the internal facies (Fig. 8) (Bolós et al., 2020).

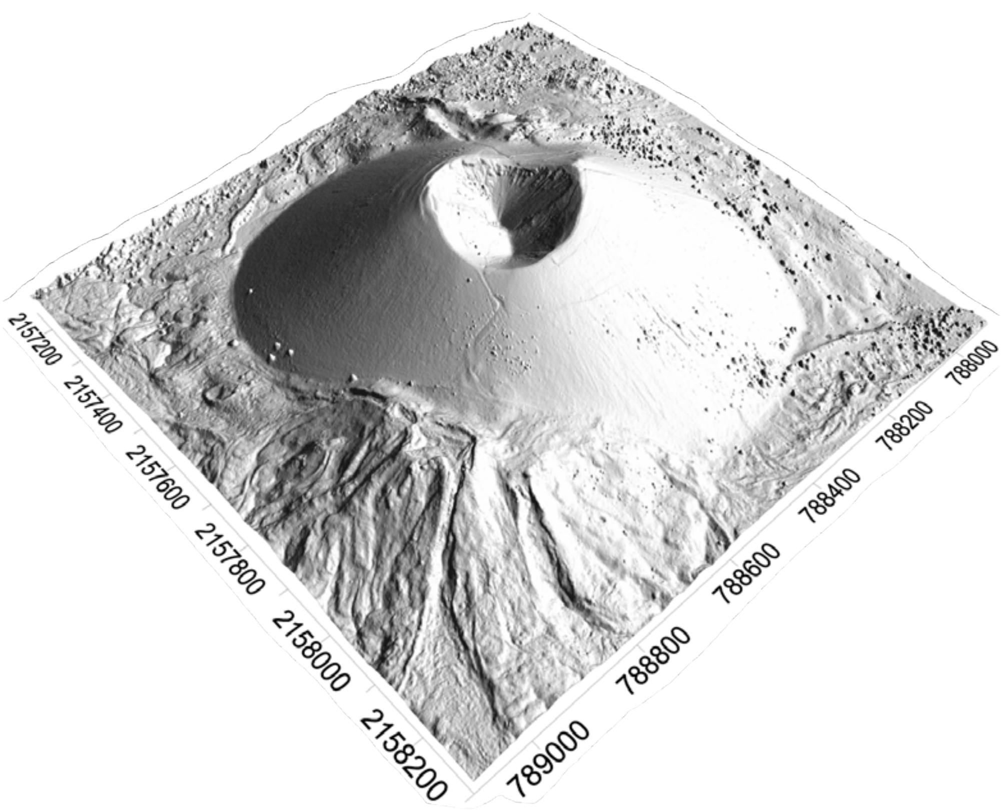

Figure 7: High-resolution DEM (36.4 cm/pixel) of the Parícutin cone (Bolós et al., 2020).

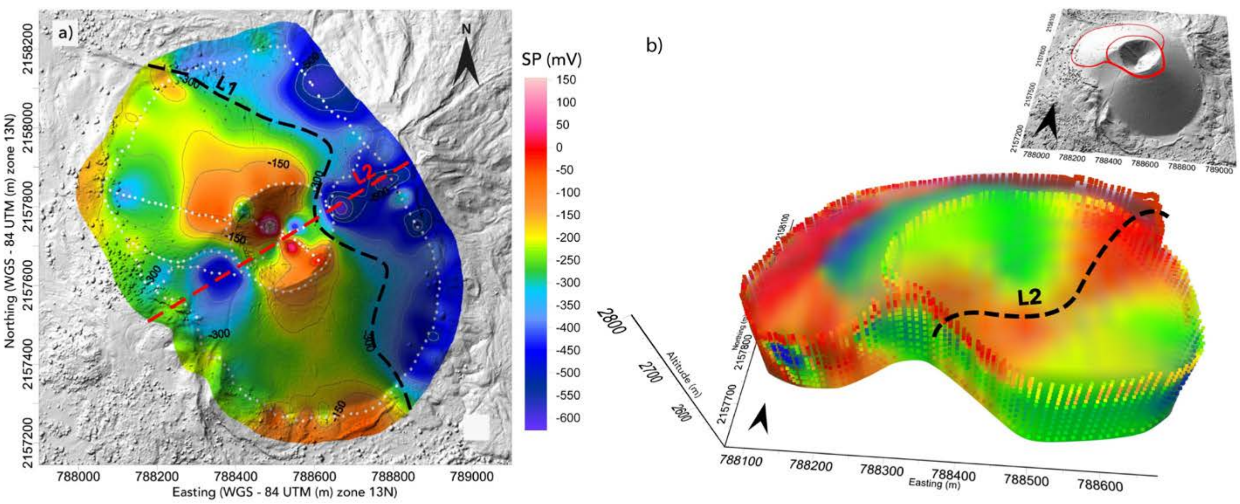

Figure 8: a) Self-potential map displaying the L1 and L2 inferred lineaments of figure 6 (Bolós et al., 2020). b) Three-dimensional resistivity model of Parícutin volcano over the topographic surface up to a surveyed depth of 95 m. Coordinates in meters (UTM 13N-WGS84). (Bolos et al., 2020).

The path along the crater rim (Stop 2) (Fig. 9) provides an overview of the lava flow-field and the surrounding area. The high density of young scoria cones in the region surrounding the Parícutin is spectacular. From the rim, it is possible to distinguish several different lava branches that piled up with time.

Figure 9: Drone view of the Parícutin crater rim (photo by Claudio Tinoco).

As during the Jorullo eruption (Guilbaud et al., 2009) the flows that reached the furthest distance from the vent were the earliest produced, because of the increase in the magma's silica content and thus viscosity with time. From the NE rim looking north, notice the Sapichu vent (from *Zapicho*, Tarascan word for kid or small boy, Ordóñez, 1947) (Fig. 5). This vent, built 8 months after the beginning of the eruption, emitted lava continuously during its 2.5 months of activity. It thus never formed a complete cone but an irregular-shaped edifice. The lava field of Parícutin is wide and it has been divided in 22 phases according to Becerril et al. (2021), slightly modified from Luhr et al. (1993) and Larrea et al. (2017) (Fig. 10).

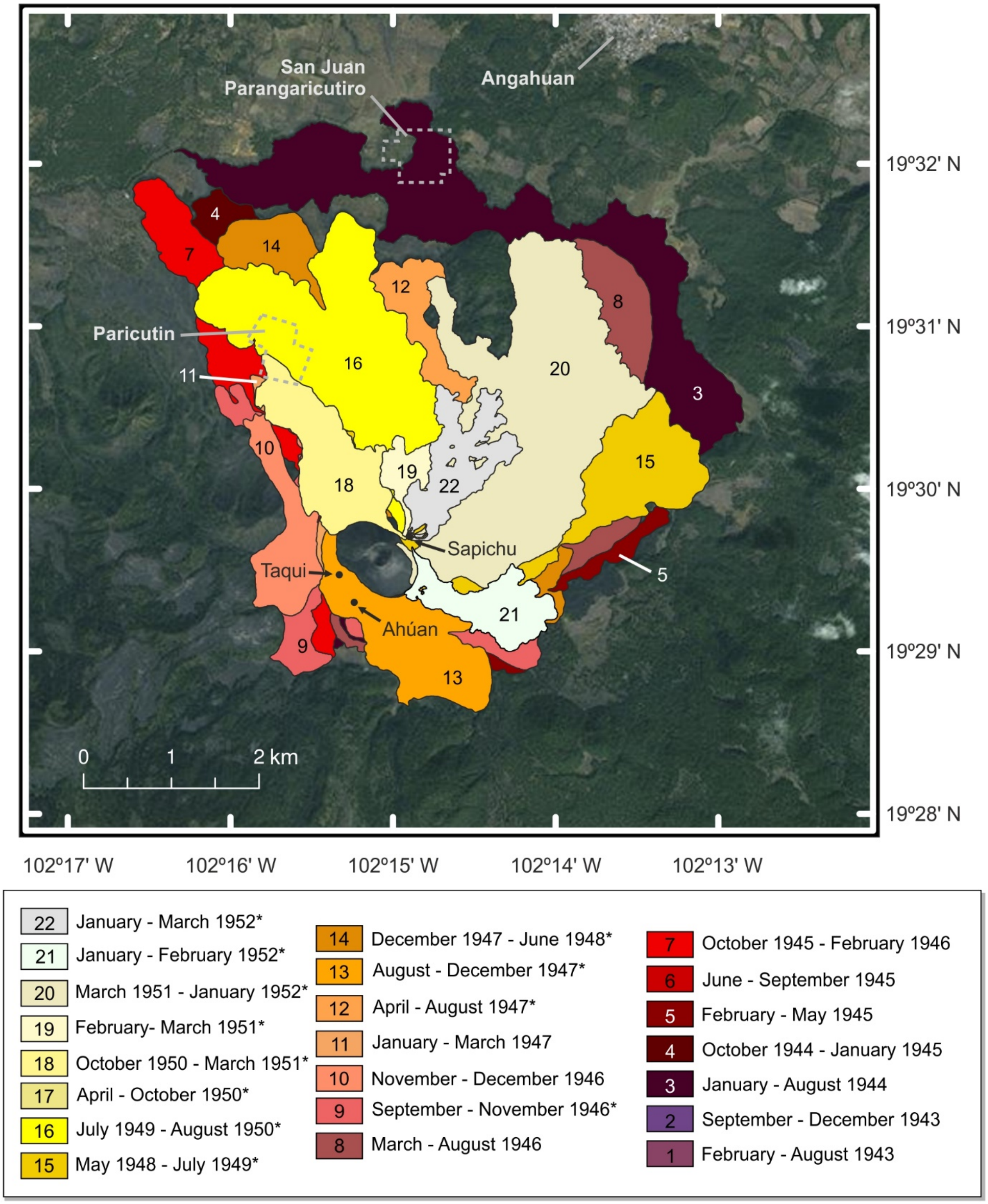

Figure 10 - Geological map of Parícutin volcano with the 22 lava eruptive phases described by Becerril et al. (2021), slightly modified from Luhr and Simkin (1993) and Larrea et al. (2017) in terms of duration, to include in one single eruptive phase the entire emplacement of each lava flow, from its initiation to its end (the modified eruptive phases are denoted in the legend with an asterisk). Location of the most active vents during the eruption are also shown (i.e., Parícutin main cone, Sapichu, Taqui, and Ahuán). Note lava eruptive phases 1, 2, 6, and 17 are not exposed on the surface because they were covered by the most recent lava flows.

Fumarole gases still escape from the Sapichu and the summit of the Parícutin cone, forming whitish coatings. Other hot fumarolic areas in the dark-colored flow-field can be seen from the crater rim, distinguishable by their contrasting whitish coloration. A 270 °C fumarole sampled in June 1995 contained 47 mol-% CO_2 and 52 mol-% air (water free basis). The carbon-13 isotope value of –20.5 ‰ for the CO_2 indicates that the hot interior of the flow was still thermally decomposing organic debris near the flow base 50 years after eruption (Goff and McMurtry, 2000). More recently, the measured conductivities across the fumarolic activity of the cone, detected several meter-scale zones of convective hydrothermal- fluid circulation of meteoric water within the cone (Bolós et al., 2020).

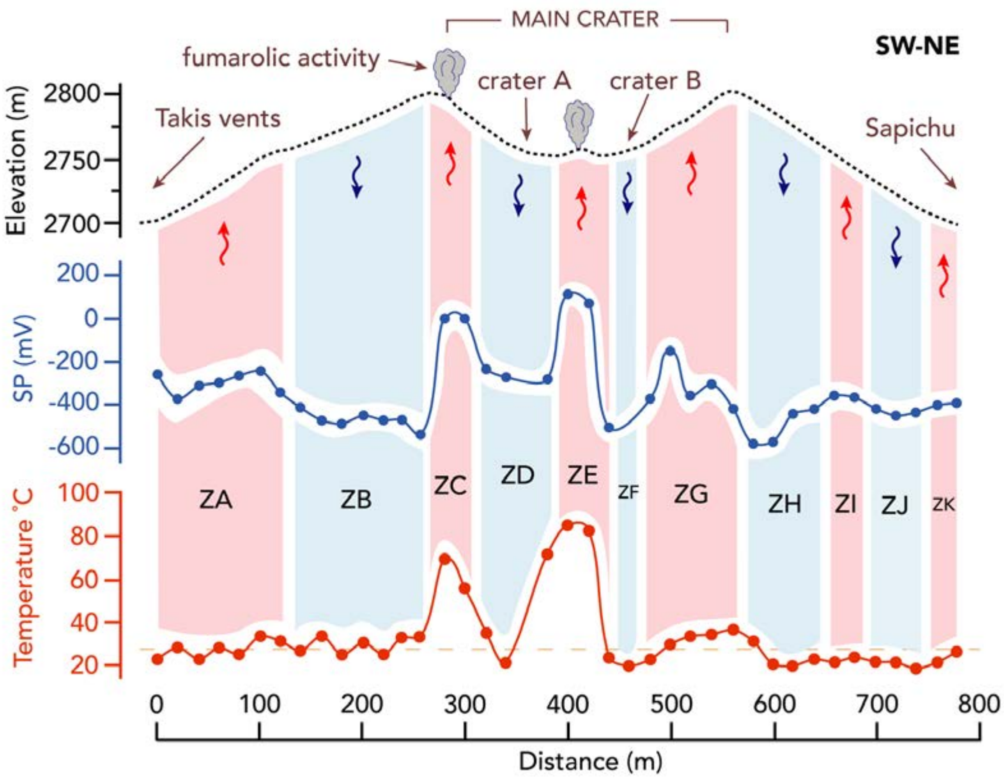

Figure 11: The topographic profile of Parícutin cone comparing the self-potential and temperature data. The preferential direction movement of the fluids is shown in blue color for the downflow and red color for the upflow (ZA-ZK). Notice the matching between the self-potential and temperature anomalies (Bolós et al., 2020).

Going back to Angahuan, we get to the third stop that is an outcrop of ash layers along the trail (Fig. 4). There, we have the opportunity to watch and discuss the stratigraphic record of fall deposits of the most explosive phases of the eruption in an open pit. This stratigraphic succession shows seven units that resulted from reworked processes, which was induced by short episodes of heavy rainfall, followed by severe dust storms during dry periods (Segerstrom, 1950, 1960). The deposits reworked by water comprise massive, grain-supported layers, interbedded with fine-grained, indurated poorly to moderately sorted laminae, and in some units the presence of raindrop marks and mud cracks at the top suggests that torrential rain events were followed by dry periods (Bolós et al., 2021). During these dry periods, wind produced ripples and dunes (Fig. 12). The analysis of these deposits reveals that more than 70% of the total thicknesses of ash around the volcano correspond to syn-eruptive reworked deposits (Bolós et al., 2021) (Fig. 13).

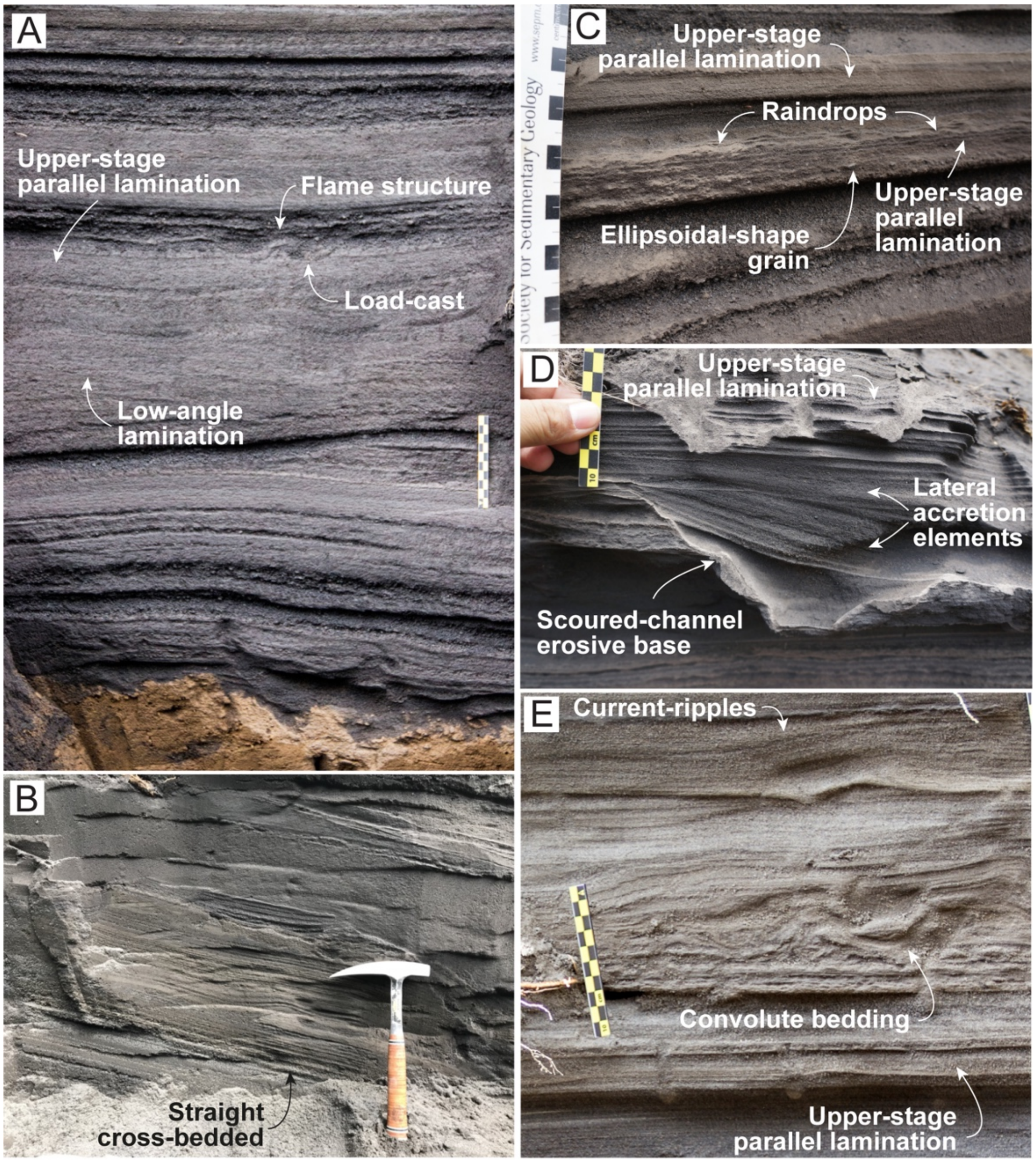

Figure 12: Photograph of the main sedimentary structures observed in the reworked deposits. A) Low-angle lamination, upper-stage parallel lamination, load-cast and flame structures as a result of humid and soft-sedimentary deformation. B) Straight cross-bedding produced by the migration of aeolian dunes with transverse morphology. C) Ellipsoidal grains oriented within upper-stage parallel lamination and raindrops. D) Upper-stage parallel lamination cut by a scoured-channel with an erosive base and filled with side accretion elements. E) Upper-stage parallel lamination, convolute bedding, and current-ripples. (Bolós et al., 2021).

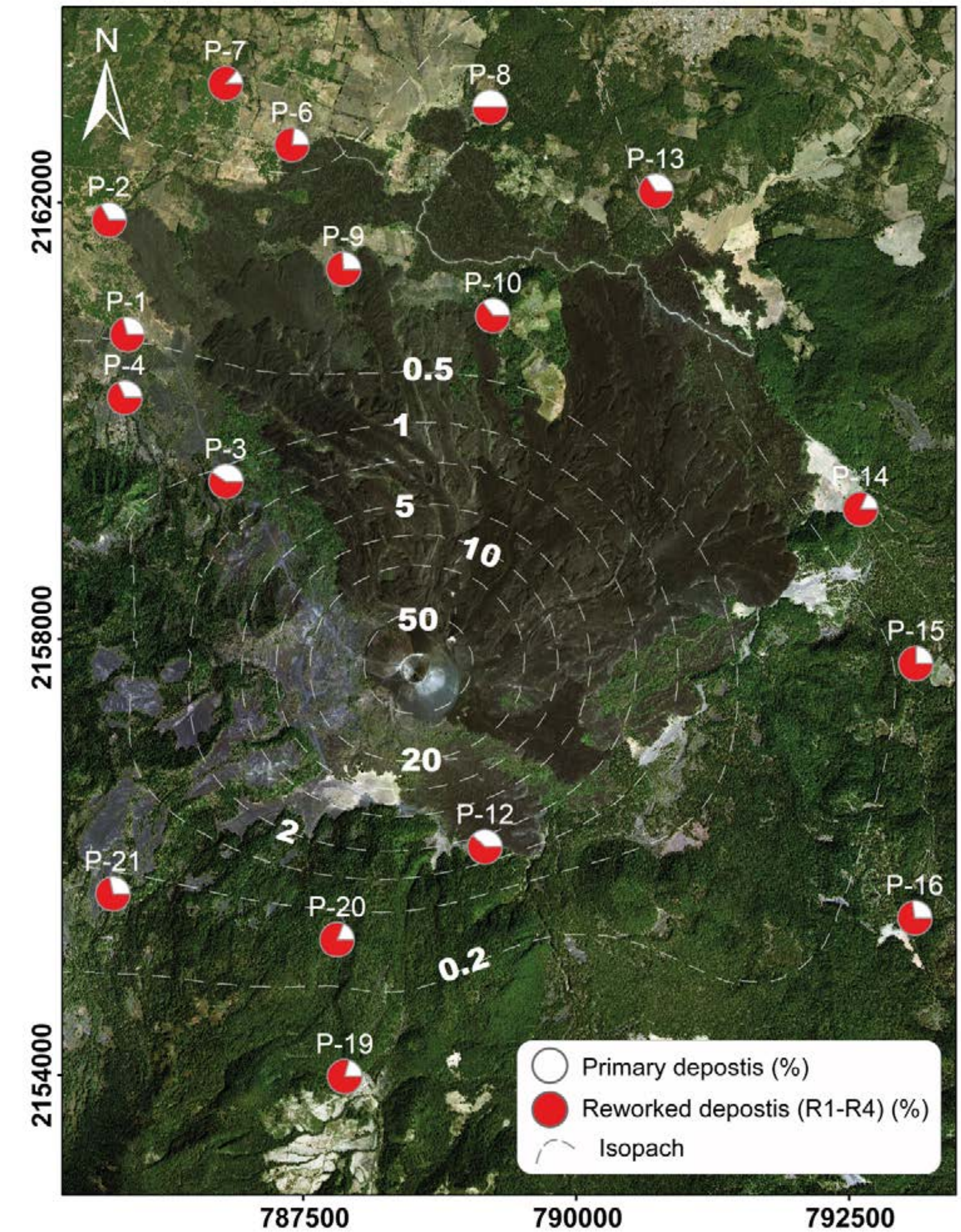

Figure 13: Model of the isopach map for isopachs between 50 m and 0.1 m in thickness, calculated for the pyroclastic deposits over the orthophotomap, also showing the location and relative proportions of pyroclastic and the interbedded reworked deposits in terms of thickness percentage (Bolós et al., 2021). Coordinates in meters (UTM 13N—WGS84).

Finally, we will make a final stop at the old church of San Juan Parangaricutiro (Fig. 14) which was buried by lava on the 19th of June 1944 (Luhr et al., 1993). At that time, it was the main town of the region with 1895 inhabitants. The conservation of the columns of the church is remarkable. Note its incomplete southern column, which was never finished, since its construction was interrupted by the activity of the Parícutin volcano. People from this town were evacuated and relocated in Nuevo San Juan. We will follow a path around the lava field at this site, which shows a strongly irregular topography and a peculiar surface texture, transitional between the pahoehoe and aa types.

Figure 14: Ruins of the church of San Juan Parangaricutiro.

Before trotting back to Angahuan and on the bus to return to Morelia, we will have the opportunity to enjoy the most delicious “quesadillas” (cheese-filled tacos) in the world while enjoying the sunset.

Recommendations

This excursion lasts approximately 10 hours (round trip), so good physical condition is required. It is however not mandatory to have previous experience of horse riding.

Please bring with you:

- 2 liters of water (minimum).
- Breakfast: Note that we will leave early from Morelia and you may have to buy something for your breakfast the previous days.
- Lunch: lunch will be provided, but it is recommended to bring something else: energy bars/fruit/nuts/chocolates (optional).
- Boots.
- Cap or hat.
- Sunglasses.

- Sunscreen.
- Sweatshirt/jacket.
- Pants and preferably a long-sleeved shirt (no shorts).
- Buff/scarf or mask to protect from the sun and ash (optional)
- Gloves to protect hands from rock abrasion and horse's reins (optional).
- A bit of cash to buy succulent local food and souvenirs from this culturally-rich region (optional).

References

Albert, H., Larrea, P., Costa, F., Widom, E., & Siebe, C. (2020). Crystals reveal magma convection and melt transport in dyke-fed eruptions. Scientific Reports, 10(1), 11632.

Becerril, L., Larrea, P., Salinas, S., Mossoux, S., Ferrés, D., Widom, E., Siebe, C. & Martí, J. (2021). The historical case of Parícutin volcano (Michoacán, México): challenges of simulating lava flows on a gentle slope during a long-lasting eruption. Natural Hazards, 107, 809-829.

Bolós, X., Macías, JL., Ocampo-Diaz, Y. Z. & Tinoco, C. (2021). Implications of reworking processes on the tephra distribution during volcanic eruptions: The case of Parícutin (1943-1952, western Mexico). Earth Surface Processes and Landforms. https://doi.org/10.1002/esp.5222

Bolós, X., Delgado-Torres, A., Cifuentes, G., Macías, J. L., Boijseauneau-López, M., Tinoco, C., & Salguero, D. (2020). Internal structure and hydrothermal fluid circulation of Parícutin volcano, Mexico: Insights gained from near-surface geophysics. Geophysical Research Letters, 47(16), e2020GL089270.

Cebriá, J. M., Martiny, B. M., López-Ruiz, J., & Morán-Zenteno, D. J. (2011). The Parícutin calc-alkaline lavas: New geochemical and petrogenetic modelling constraints on the crustal assimilation process. Journal of Volcanology and Geothermal Research, 201(1-4), 113-125.

Erlund, E. J., Cashman, K. V., Wallace, P. J., Pioli, L., Rosi, M., Johnson, E., & Granados, H. D. (2010). Compositional evolution of magma from Parícutin Volcano, Mexico: The tephra record. Journal of Volcanology and Geothermal Research, 197(1-4), 167-187.

Foshag, W. F., & González-Reyna, J. (1956). Birth and development of Parícutin volcano, Mexico. USGS Bull, 355-489.

Fries Jr, C. (1953). Volumes and weights of pyroclastic material, lava, and water erupted by Parícutin volcano, Michoacan, Mexico. Eos, Transactions American Geophysical Union, 34(4), 603-616.

Gardine, M., West, M. E., & Cox, T. (2011). Dike emplacement near Parícutin volcano, Mexico in 2006. Bull. Volcanol. 73: 123-132.

Goff, F., & McMurtry, G. M. (2000). Tritium and stable isotopes of magmatic waters. Journal of Volcanology and Geothermal Research, 97(1-4), 347-396.

Guilbaud, M. N., Siebe, C. & Salinas, S. (2009). Excursions to Parícutin and Jorullo (Michoacán), the youngest volcanoes of the Trans-Mexican Volcanic Belt. Impretei, México D.F., 31 p.

Hasenaka, T., & Carmichael, I. S. (1985). The cinder cones of Michoacán—Guanajuato, central Mexico: Their age, volume and distribution, and magma discharge rate. Journal of Volcanology and Geothermal Research, 25(1-2), 105-124.

Jácome-Paz, M. P., Delgado-Granados, H., Pérez-Campos, X., Espinasa-Pereña, R., & Campion, R. (2022). Diffuse degassing baseline in Parícutin volcano and Michoacán-Guanajuato monogenetic volcanic field, México. Journal of Volcanology and Geothermal Research, 425: 107534.

Larrea, P., Albert, H., Ubide, T., Costa, F., Colás, V., Widom, E., & Siebe, C. (2021). From explosive vent opening to effusive outpouring: mineral constraints on magma dynamics and timescales at Parícutin monogenetic volcano. Journal of Petrology, 62(4), egaa112.

Larrea, P., Salinas, S., Widom, E., Siebe, C., & Abbitt, R. J. (2017). Compositional and volumetric development of a monogenetic lava flow field: The historical case of Parícutin (Michoacán, Mexico). Journal of Volcanology and Geothermal Research, 348, 36-48.

Larrea, P., Widom, E., Siebe, C., Salinas, S., & Kuentz, D. (2019). A re-interpretation of the petrogenesis of Parícutin volcano: Distinguishing crustal contamination from mantle heterogeneity. Chemical Geology, 504, 66-82.

Luhr, J. F. (2001). Glass inclusions and melt volatile contents at Parícutin Volcano, Mexico. Contributions to Mineralogy and Petrology, 142(3), 261-283.

Luhr, J. F., Simkin, T., & Cuasay, M. (1993). Parícutin: the volcano born in a Mexican cornfield. In Parícutin: The volcano born in a Mexican cornfield. US Geoscience Press.

MacDonald, G. A. (1972). Volcanoes. Prentice Hall, 510 p.

McBirney, A. R., Taylor, H. P., Armstrong, R. L. (1987). Parícutin re-examined: a classic example of crustal assimilation in calc-alkaline magma. Contributions to Mineralogy and Petrology 95: 4-20.

Mahgoub, A. N., Böhnel, H., Siebe, C., Salinas, S., & Guilbaud, M. N. (2017). Paleomagnetically inferred ages of a cluster of Holocene monogenetic eruptions in the Tacámbaro-Puruarán area (Michoacán, México): implications for volcanic hazards. Journal of Volcanology and Geothermal Research, 347, 360-370.

Ownby, S., Granados, H. D., Lange, R. A., & Hall, C. M. (2007). Volcán Tancítaro, Michoacán, Mexico, $^{40}Ar/^{39}Ar$ constraints on its history of sector collapse. J Volcanol Geotherm Res 161(1):1–14.

Ordoñez, E. (1947). El volcán Paricutín: México. Editorial Fantasía.

Rowe, M. C., Peate, D. W., & Ukstins Peate, I. (2011). An investigation into the nature of the magmatic plumbing system at Parícutin Volcano, Mexico. Journal of Petrology, 52(11), 2187-2220.

Segerstrom, K. (1950). Erosion studies at Parícutin, state of Michoacán, Mexico US Geological Survey No. 965-A, 1-151.

Segerstrom, K. (1960). Erosion and related phenomena at Parícutin in 1957. US Geological Survey Bulletin 1104A, 1-18.

Pioli, L., Erlund, E., Johnson, E., Cashman, K., Wallace, P., Rosi, M., & Granados, H. D. (2008). Explosive dynamics of violent Strombolian eruptions: the eruption of Parícutin Volcano 1943–1952 (Mexico). Earth and planetary science letters, 271(1-4), 359-368.

Siebe, C., Guilbaud, M. N., Salinas, S., Kshirsagar, P., Chevrel, M. O., de la Fuente, J. R., Hernández-Jiménez, A., & Godínez, L. (2014). Monogenetic volcanism of the Michoacán-Guanajuato Volcanic Field: Maar craters of the Zacapu basin and domes, shields, and scoria cones of the Tarascan highlands (Paracho-Parícutin region). Fieldguide, pre-meeting fieldtrip (Nov. 13-17) for the 5th International Maar Conference (5IMC-IAVCEI), Querétaro, México, 33 p.

Valentine, G. A., & Connor, C. B. (2015). Basaltic volcanic fields. In: The Encyclopedia of Volcanoes, Second edition. pp. 423–439.

Wilcox, R. E. (1954). Petrology of Parícutin Volcano, Mexico. US Geo. Surv. Bull.

ANNIVERSARY OF
PARÍCUTIN VOLCANO